Proceedings of the VIIIth International Workshop on Heavy Quarks and Leptons HQL06

October 2006

Deutsches Museum, Munich

Editors
S. Recksiegel, A. Hoang, S. Paul

Organized by the Physics Department of the Technical University of Munich
and the Max-Planck Institute for Physics, Munich

Semileptonic b to u transition

Eunil Won
Department of Physics
Korea University
136-713 Seoul, Korea

1 Introduction

The parameter $|V_{ub}|$ is one of the smallest and least known elements of the Cabibbo-Kobayashi-Maskawa (CKM) quark-mixing matrix. A precise determination of $|V_{ub}|$ would significantly improve the constraints on the unitarity triangle and provide a stringent test of the Standard Model mechanism for CP violation. With the CKM angle ϕ_3, $|V_{ub}|$ can constrain the unitarity triangle from tree level processes alone.

Experimental studies of charmless semileptonic B decays can be broadly categorized into inclusive and exclusive measurements depending on how the final states are treated. The inclusive method measures the decay rate $\Gamma(B \to X_u \ell\nu)$, where X_u is known as the hadronic system that does not contain charm-quark. On the other hand, the exclusive method measures the decay rates for exclusive final states such as $B \to \pi\ell\nu$ and $\rho\ell\nu$. Two methods give not only different efficiencies and signal-to-background ratios, but also different theoretical calculations to be used in order to extract $|V_{ub}|$. Using both approaches and comparing the results will help us verify the robustness of the theoretical error estimation, which dominates the current uncertainty in the determination of $|V_{ub}|$. Progress in last few years will be summarized in this presentation.

2 Inclusive determination of $|V_{ub}|$

The inclusive semileptonic decay rates in the quark level depend only on CKM matrix element and the quark mass, as shown in the following equation

$$\Gamma(b \to u\ell\overline{\nu}) = \frac{G_F^2}{192\pi^2}|V_{ub}|^2 m_b^5 \tag{1}$$

where G_F is the Fermi constant and m_b is the b-quark mass. The hadronic level is easy to calculate with the framework of operator product expansion (OPE) [1] and

the $|V_{ub}|$ can be parametrized as

$$|V_{ub}| = 0.00424 \left\{ \frac{\mathcal{B}(B \to X_u \ell\nu)}{0.02} \frac{1.61\text{ps}}{\tau_b} \right\}^{\frac{1}{2}} \times (1.0 \pm 0.012_{\text{QCD}} \pm 0.022_{\text{HQE}}) \qquad (2)$$

where the first error comes from the uncertainty in the calculation of quantum chromodynamics (QCD), perturbative and non-perturbative quantities and the 2nd from the uncertainty in the heavy quark expansion (HQE), sensitive to m_b. This formulation [2] has been updated in ICHEP06. The main problem in the inclusive method is the background from the b to c decays because the rate is approximately 50 times larger, namely

$$\Gamma(b \to c\ell\nu) \sim 50\Gamma(b \to u\ell\nu). \qquad (3)$$

One may attempt to remove this large background by applying kinematic selection criteria but once the signal to background ratio becomes controllable, the OPE is known to fail in such limited phase space. In the theory side, in order to overcome this problem, various different techniques have been developed. For example, a non-perturbative shape function [3] (SF) is developed to extrapolate to the full phase space. The shape function is the lightcone momentum distribution function of the b-quark inside the meson. The detailed shape is not known theoretically from the first principle and even phenominologically, the low-tail part is least known. The shape function is needed to be determined from experimental data. The other approach is called dressed gluon exponentiation (DGE) [4] according to the factorization properties of the fully differential width in inclusive decays Sudakov logarithms exponentiate in moment space. The third approach [5] measures the ratio of $|V_{ub}|/|V_{ts}|$ with the photon energy spectrum in $b \to s\gamma$ decay mode. This technique is interesting as the only residual shape function dependence remain at the end.

- Lepton Endpoint Analysis

The theoretical calculations allow for the extraction of the observed partial $B \to X_u \ell\nu$ decay rate above a certain lepton momentum to the total inclusive $B \to X_u \ell\nu$ decay rate using the measured shape function parameters and a subsequent translation of the total decay rate to $|V_{ub}|$. The experimental study was pioneered by the CLEO collaboration [6] and the recent work was carried out by the BaBar collaboration [7]. Fig. 1 (a), (b), and (c) show the electron energy spectra for various cases. Open circles in Fig. 1 (a) show the on-resonance data and closed circles with a curve in Fig. 1 (a) show the off-resonance data where non-$B\overline{B}$ background is included. The triangles in Fig. 1 (b) show the data after the non $B\overline{B}$ background subtraction and the histogram in Fig. 1 (b) show the simulated $B\overline{B}$ background. Closed squares and the histogram in Fig. 1 (c) show the data and the simulated signal after all background subtraction,

respectively. It is obvious that the subtraction of backgrounds is extremely crucial in this kind of analysis. The shaded region in Fig. 1 (c) is used for the final extraction of the $|V_{ub}|$. In the mean time, the partial branching fraction can be obtained from the background subtracted data and the summary from three experiment is listed in Table 1. Note that the Belle's result has the lowest cut on E_ℓ.

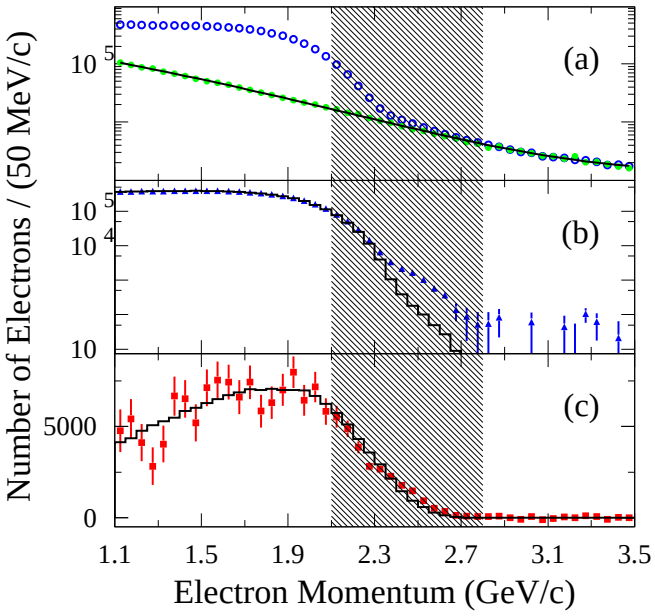

Figure 1: The distribution of electron momentum is shown [7]. Open circles in (a) show the on-resonance data and closed circles with a curve in (a) show the off-resonance data where non-$B\overline{B}$ background is included. The triangles in (b) show the data after the non $B\overline{B}$ background subtraction and the histogram (b) show the simulated $B\overline{B}$ background. Closed squares and the histogram in (c) show the data and the simulated signal after all background subtraction, respectively.

- Measurements of m_X, P_+, and q^2

In this analysis, the measurements are made with a sample of events where the hadronic decay mode of the tagging side B meson, B_{tag}, is fully reconstructed, while the semileptonic decay of the signal side B meson, B_{sig}, is identified by the presence of a high momentum electron or muon. B denotes both charged and neutral B mesons. This method allows the construction of the invariant masses of the hadronic (M_X) and leptonic ($\sqrt{q^2}$) system in the semileptonic decay, and the variable $P_+ =$

Table 1: Summary of the partial branching fraction of $B \to X_u \ell\nu$ given the lepton energy cut.

data	$\Delta\mathcal{B}(10^{-4})$	E_l (GeV)
CLEO 9/fb	$2.30 \pm 0.15 \pm 0.35$	2.1
Belle 27/fb	$8.47 \pm 0.37 \pm 1.53$	1.9
BaBar 80/fb	$5.72 \pm 0.41 \pm 0.65$	2.0

$E_X - |\vec{p}_X|$ where E_X is the energy and $|\vec{p}_X|$ the magnitude of the three-momentum of the hadronic system. These inclusive kinematic variables can be used to separate the $B \to X_u \ell\nu$ decays from the much more abundant $B \to X_c \ell\nu$ decays. Three competing kinematic regions were proposed by theoretical studies [3,8], based on the three kinematic variables, and are directly compared by this analysis.

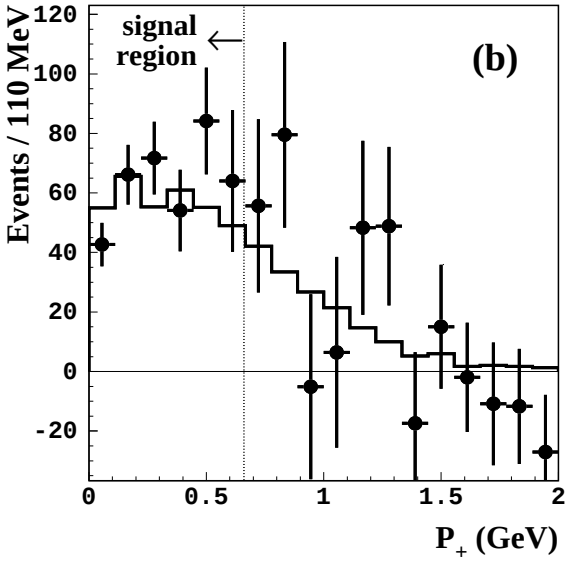

Figure 2: The P_+ distribution (symbols with error bars) after subtracting $B \to X_c \ell\nu$ background, with fitted $B \to X_u \ell\nu$ contribution (histogram).

The value of $|V_{ub}|$ is extracted using recent theoretical calculation [3,8] that include all the current known contributions. Results from the Belle experiment using a data set of 253/fb [9] is the first one to use P_+. Figure 2 show the distribution of the variable P_+. Signal region is defined by $P_X < 0.66$ GeV and shows a clear indication of enhancement of the signal in Fig. 2. BaBar did also similar analysis but only with M_X and q^2 [10]. The measured partial branching fractions from both experiments for different phase space values are summarized in Table 2. Note that the errors are

Table 2: Summary of the partial branching fraction of $B \to X_u \ell\nu$ given the lepton energy cut.

data	Phase Space	$\Delta\mathcal{B}$ (10^{-4})
Belle 253/fb	$M_X < 1.7$	$12.4 \pm 1.1 \pm 1.0$
	$M_X < 1.7$, $q^2 > 8$	$8.4 \pm 0.8 \pm 1.0$
	$P_+ < 0.66$	$11.0 \pm 1.0 \pm 1.6$
BaBar 211/fb	$M_X < 1.7$, $q^2 > 8$	$8.7 \pm 0.9 \pm 0.9$ (preliminary)

larger than those appeared in the endpoint analyses results.

- Extraction of $|V_{ub}|$

In order to extract the $|V_{ub}|$ from the partial branching fraction measurements described so far, one has to know the distribution of the shape function. The photon energy spectrum in $B \to X_s\gamma$ provides access to such distribution function of the b quark inside the B meson [11]. The knowledge of this shape function is a crucial input to the extraction of $|V_{ub}|$ from inclusive semileptonic $B \to X_u\ell\nu$ measurements. Both Belle and Babar fit the spectrum to theoretical predictions in order to extract the $|V_{ub}|$.

Using the heavy quark parameter values $m_b(\mathrm{SF}) = 4.60 \pm 0.04$ GeV and $\mu_\pi^2(\mathrm{SF}) = 0.20 \pm 0.04$ GeV^2, the value of $|V_{ub}|$ from various experimental results is extracted within "BLNP" framework [3]. This is done by the heavy flavour averaging group [12] (HFAG) and the result is

$$|V_{ub}|_{\mathrm{BLNP}} = (4.49 \pm 0.19_{\mathrm{exp}} \pm 0.27_{\mathrm{theory}}) \times 10^{-3}. \quad (4)$$

Note that the total error in percentage is

$$\delta|V_{ub}|_{\mathrm{BLNP}} = \pm 7.3\% \quad (5)$$

and the result indicates that the precision of the measurement is still limited by theoretical uncertainty but the value of the error is not far from the experimental error. The individual result from experiments is shown in Fig. 3. Note that the best measurement is from the endpoint analysis at present. Contributions to the experimental and theoretical errors can be found in Table 3. The contribution from sub-leading SF, for example, is known to be hard to reduce from the present value.

One can also extract $|V_{ub}|$ using the DGE framework [4]. This is also done by HFAG and the result is

$$|V_{ub}|_{\mathrm{DGE}} = (4.46 \pm 0.20_{\mathrm{exp}} \pm 0.20_{\mathrm{theory}}) \times 10^{-3}. \quad (6)$$

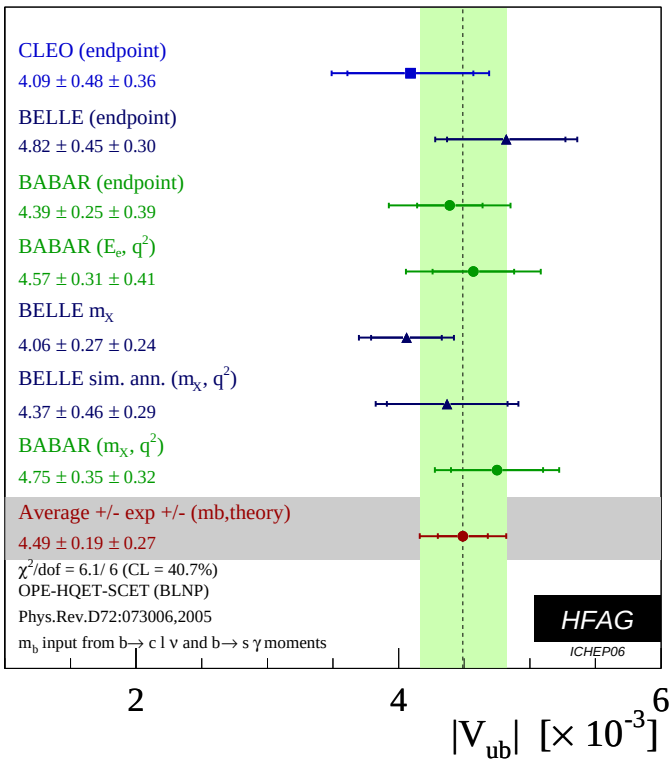

Figure 3: Summary of the measurements of $|V_{ub}|$ within BLNP framework from various experiments are shown. The averaged value is $|V_{ub}|_{\rm BLNP} = (4.49 \pm 0.19_{\rm exp} \pm 0.27_{\rm theory}) \times 10^{-3}$.

with the parameter $m_b(\overline{\rm MS}) = 4.20 \pm 0.04$ GeV. Note that the result is in good agreement with the result with BLNP method, and is remarkable as two theoretical methods use rather different approach in their calculations. The contribution of the error is also listed in Table 4. The sharing of the error is also similar to the case of the BLNP framework. One thing to note is that the weak annihilation is not taken into account in this case.

On the other hand, BaBar explored alternative methods in obtaining $|V_{ub}|$. Leibovich, Low, and Rothstein (LLR) [5] have presented a prescription to extract $|V_{ub}|$ with reduced model dependence from either the lepton energy or the hadronic mass m_X [13]. The calculations of LLR are accurate up to corrections of order α_s^2 and $(\Lambda m_B/(\zeta m_b))^2$, where ζ is the experimental maximum hadronic mass up to which the $B \to X_u \ell \nu$ decay rate is determined and $\Lambda \sim \Lambda_{\rm QCD}$. This method combines the hadronic mass spectrum, integrated below ζ, with the high-energy end of the measured differential $B \to X_s \gamma$ photon energy spectrum via the calculations of LLR. The measured $|V_{ub}|$ as a function of ζ is shown in Fig. 4. The small arrow indicates the

Table 3: Summary of the contributions to the experimental and theoretical errors of $|V_{ub}|$ in the BLNP framework.

Source	contribution (%)
statistical	2.2
Expt. systematic	2.8
$b \to c\ell\nu$ model	1.9
$b \to u\ell\nu$ model	1.6
HQ parameters	4.2
sub-leading SF	3.8
Weak Annihilation	1.9

Table 4: Summary of the contributions to the experimental and theoretical errors of $|V_{ub}|$ in the DGE framework.

Source	contribution (%)
statistical	1.8
Expt. systematic	2.5
$b \to c\ell\nu$ model	2.3
$b \to u\ell\nu$ model	2.3
m_b (R_CUT)	1.2
α_s (R_CUT)	1.0
Total semiloptonic width	3.0
DGE theory	2.9

value of ζ that is used for the cut, $\zeta = 0.67$ GeV/c^2. At this point, the measured value becomes

$$|V_{ub}| = (4.43 \pm 0.38_{\rm stat} \pm 0.25_{\rm syst} \pm 0.29_{\rm th}) \times 10^{-3}. \quad (7)$$

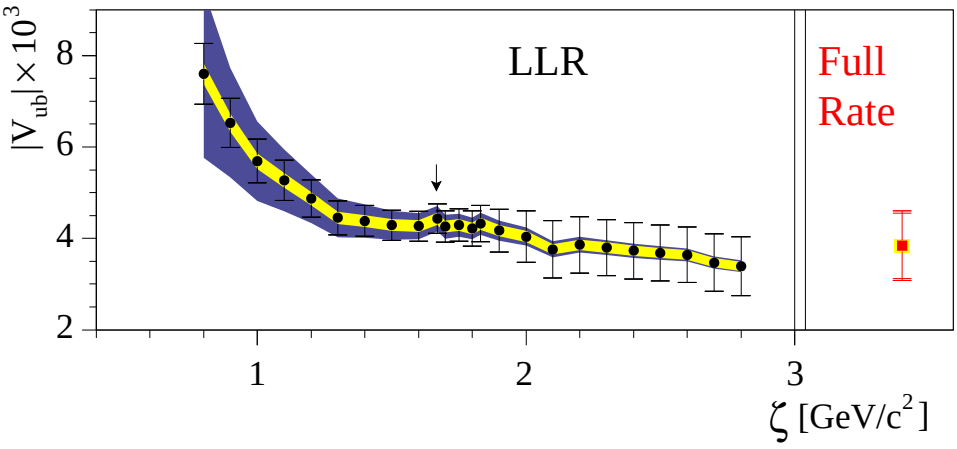

Figure 4: $|V_{ub}|$ as a function of ζ with the LLR method (left) and for the determination with the full rate measurement (right). The error bars indicate the statistical uncertainty. They are correlated between the points and get larger for larger ζ due to larger background from $B \to X_c \ell\nu$. The total shaded are illustrates the theoretical uncertainty; the inner light shaded area indicates the perturbative share of the uncertainty. The arrow indicates $\zeta = 1.67$ GeV/c^2.

Another approach that BaBar chooses to reduce the model dependence is to measure the $B \to X_u \ell\nu$ rate over the entire M_X spectrum. Since no extrapolation is necessary to obtain the full rate, systematic uncertainties from m_b and Fermi motion are much reduced. Perturbative corrections are known to order α_s. The rate of $B \to X_u \ell\nu$ is extracted from the hadronic mass spectrum up to $\zeta = 2.5$ GeV/c^2 which corresponds to about 96 % of the simulated hadronic mass spectrum, and find $|V_{ub}| = (3.84 \pm 0.70_{\rm stat} \pm 0.30_{\rm syst} \pm 0.10_{\rm th}) \times 10^{-3}$, using the average B lifetime of $\tau_B = (1.604 \pm 0.012)$ ps. The current uncertainties on the $B \to X_s\gamma$ photon energy spectrum limit the sensitivity with which the behavior at high ζ can be probed. These two new results are consistent with previous measurements but have substantially smaller uncertainties from m_b and the modeling for Fermi motion of the b quark inside the B meson. Both techniques are based on theoretical calculations that are distinct from other calculations normally employed to extract $|V_{ub}|$ and, thus, provide a complementary determination of $|V_{ub}|$.

3 Exclusive determination of $|V_{ub}|$

In this section, we discuss the extraction of $|V_{ub}|$ from exclusive decays such as $B \to (\pi, \rho, \omega)\ell\nu$. For $B^0 \to \pi^-\ell^+\nu$ decays, the differential decay rate becomes

$$\frac{d\Gamma(B \to \pi\ell\nu)}{dq^2} = \frac{G_F^2}{24\pi^3}|V_{ub}|^2 p_\pi^3 |f_+(q^2)|^2 \tag{8}$$

where $f_+(q^2)$ is a form factor and q^2 is the squared invariant mass of the $\ell^+\nu$ system. Only shape of $f_+(q^2)$ can be measured experimentally. Its normalization is provided by theoretical calculations which currently suffer from relatively large uncertainties and, often, do not agree with each other. As a result, the normalization of the $f_+(q^2)$ form factor is the largest source of uncertainly in the extraction of $|V_{ub}|$ from the $B^0 \to \pi^-\ell^+\nu$ branching fraction. Values of $f_+(q^2)$ for $B^0 \to \pi^-\ell^+\nu$ decays are provided by unquenched [14,15] and quenched [16] lattice QCD calculations, presently reliable only at high q^2 (> 16 GeV^2/c^4), and by Light Cone Sum Rules calculations [17] (LCSR) based on approximations only valid at low q^2 (< 16 GeV^2/c^4), as well as by a quark model [18]. The QCD theoretical predictions are at present more precise for $B^0 \to \pi^-\ell^+\nu$ decays than for other exclusive $B \to X_u\ell\nu$ decays. Experimental data can be used to discriminate between the various calculations by measuring the $f_+(q^2)$ shape precisely, thereby leading to a smaller theoretical uncertainty on $|V_{ub}|$.

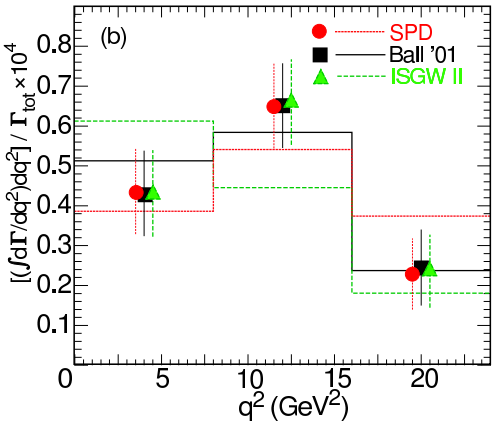

Figure 5: Fit to $d\Gamma/dq^2$ on exclusive $B \to \pi^-\ell^+\nu$ decays.

For the recoiling the other side of the B meson, we may require nothing (untagged) or require indication of semileptonic decay ($D^{(*)}\ell\nu$ tag), and require hadronic decay (full reconstruction tag). We review recent progress on experimental studies with different tagging methods listed above.

- Untagged $B \to \pi\ell\nu$

CLEO pioneered the measurement of V_{ub} with exclusive decays [19]. They perform a simultaneous maximum likelihood fit in ΔE and $M_{m\ell\nu}$ to seven sub-modes: $\pi^{\pm}$, π^0, $\rho^{\pm}$, $\omega/\eta \to pi^+\pi^-\pi^0$, and $\eta \to \gamma\gamma$. In the fit they used isospin symmetry to constrain the semileptonic widths $\Gamma^{\rm SL}(\pi^{\pm}) = 2\Gamma^{\rm SL}$ (π^0) and $\Gamma^{\rm SL}(\rho^{\pm}) = 2\Gamma^{\rm SL}$ (ρ^0) $\sim 2\Gamma^{\rm SL}$ (ω), where the final approximate equality is inspired by constituent quark symmetry. Signals for π and ρ are extracted separately in three q^2 bins. Given form factors from theory, they extracted $|V_{ub}|$ from a fit to $d\Gamma/dq^2$, and it is shown in Fig. 5. From their fit, we see that ISGW2 [18] is least favored. Combining $B \to \pi\ell\nu$ and $B \to \rho\ell\nu$ results, CLEO found that

$$|V_{ub}| = (3.17 \pm 0.17({\rm stat})^{+0.16}_{-0.17}({\rm syst})^{+0.53}_{-0.39}({\rm theo}) \pm 0.03_{\rm FF}) \times 10^{-3}. \quad (9)$$

BaBar also did similar but improved analysis [20]. More accurate value of q^2 was obtained in the so-called Y-average frame where the pseudo-particle Y has a four-momentum defined by $P_Y \equiv (P_\pi + P_\ell)$. The angle θ_{YT} between the directions of the p^*_B and p^*_Y momenta in the $\Upsilon(4S)$ rest frame can be determined assuming energy-momentum conservation in a semileptonic $B \to Y\nu$ decay. The use of the Y-averaged frame yields a q^2 resolution that is approximately 20 % bettern than what is obatined in the usual $\Upsilon(4S)$ frame where the B meson is assumed to be at rest. They also fit the $\Delta\mathcal{B}/\mathcal{B}$ spectrum using a probability density function based on the $f_+(q^2, \alpha)$ parametrization of Becirevic-Kaidalov [21] (BK). The normalized $\Delta\mathcal{B}/\mathcal{B}$ distribution is shown in Fig. 6, together with the result of a $f_+(q^2)$ shape fit using the BK parametrization and theoretical prediction. The obtain a value of $\alpha = 0.53$ $\pm$ 0.05 $\pm$ 0.04. BaBar data are clearly incompatible with the ISGW2 quark model, which is in agreement with what CLEO data indicated before. The extraction of $|V_{ub}|$ is carried out from the partial branching fractions using $|V_{ub}| = \sqrt{\Delta\mathcal{B}/(\tau^0_B \Delta\zeta)}$, where $\tau^0_B = (1.536 \pm 0.014)$ ps is the B^0 lifetime and $\Delta\zeta$ is the normalized partial decay rate predicted by various form factor calculations. For the LCSR calculations with $q^2 <$ 16 GeV^2/c^4, $|V_{ub}| = (3.6 \pm 0.1 \pm 0.1\ ^{+0.6}_{-0.4}) \times 10^{-3}$ is obtained. For the HPQCD and and FNAL lattice calculations with $q^2 >$ 16 GeV^2/c^4, $|V_{ub}| = (4.1 \pm 0.2 \pm 0.2\ ^{+0.6}_{-0.4})$ $\times 10^{-3}$ and $|V_{ub}| = (3.6 \pm 0.2 \pm 0.2\ ^{+0.6}_{-0.4}) \times 10^{-3}$ are obtained, respectively. Note that all are in good agreement within given uncertainty and this gives us confidence in exclusive measurement of $|V_{ub}|$.

- $D^{(*)}\ell\nu$ tag

Belle presented measurements of $B^0 \to \pi^-/\rho^-\ell^+\nu$ and $B^+ \to \pi^0/\rho^0\ell^+\nu$ decays using $B \to D^{(*)}\ell\nu$ tagging [22]. They reconstruct the entire decay chain from the $\Upsilon(4S)$

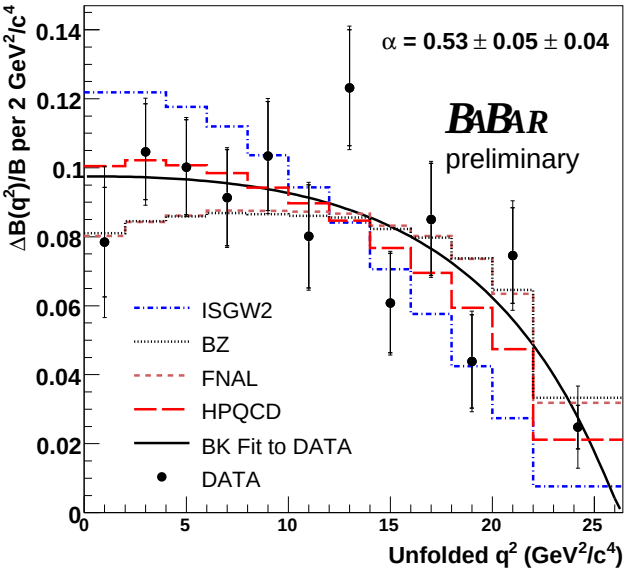

Figure 6: Differential decay rate formula fitted to the normalized partial $\Delta\mathcal{B}/\mathcal{B}$ spectrum in 12 bins of q^2. The smaller error bars are statistical only while the larger error bars include statistical and systematic uncertainties. The BK parametrization (solid black curve) reproduces the data quite well (χ^2=8.8 for 11 degrees of freedom) with the parameter $\alpha = 0.53 \pm 0.05 \pm 0.04$. The data are also compared to LCSR calculations (dotted line), unquenched LQCD calculations (long dashed line and short dashed line) and the ISGW2 quark model (dash-dot line).

$\to B_{\rm sig}B_{\rm tag}$, $B_{\rm sig} \to \pi/\rho\ell\nu$ and $B_{\rm tag} \to D^{(*)}\ell\nu$ tag with several $D^{(*)}$ sub-modes. The back-to-back correlation of the two B mesons in the $\Upsilon(4S)$ rest frame allows us to constrain the kinematics of the double semileptonic decay. The signal is reconstructed in four modes, $B^0 \to \pi^-/\rho^-\ell^+\nu$ and $B^+ \to \pi^0/\rho^0\ell^+\nu$. Yields and branching fractions are extracted from a simultaneous fit of the B^0 and B^+ samples in three intervals of q^2, accounting for cross-feed between modes as well as other backgrounds. Belle applied this methods to $B \to \pi/\rho\ell\nu$ decays for the first time, and have succeeded in reconstructing these decays with significantly improved signal-to-noise ratios compared to the ν-reconstruction method. With the data of 253 fb^{-1}, Belle extracted branching fractions and $|V_{ub}|$. Figure 7 shows the q^2 distribution for the decay $B^0 \to \pi^-/\rho^-\ell^+\nu$. The error bars are too large to reject any of form factor models for the moment. Table 5 summarized the results with two different lattice calculations. This gives about 13 % experimental uncertainty on $|V_{ub}|$, currently dominated by the statistical error of 11 %. By accumulating more integrated luminosity, a measurement with errors

Table 5: Summary of $|V_{ub}|$ measurements by the Belle collaboration with different lattice calculations.

	q^2 GeV^2/c^4	$\|V_{ub}\| \times 10^{-3}$
FNAL	> 16	$3.60 \pm 0.41 \pm 0.20 \pm {}^{0.62}_{-0.41}$
HPQCD	> 16	$4.03 \pm 0.46 \pm 0.22 \pm {}^{0.59}_{-0.41}$

below 10 % is feasible. With improvements to unquenched LQCD calculations, the present method may provide a precise determination of $|V_{ub}|$.

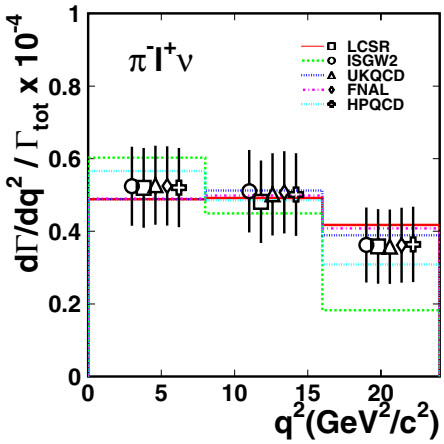

Figure 7: Extracted q^2 distribution for $B^0 \to \pi^- \ell^+ \nu$ decays. Data points are shown for different form factor models used to estimate the detection efficiency. Lines are for the best fit of the form factor shapes to the obtained q^2 distribution.

The BaBar collaboration also did similar analysis [23] based on 211 fb^{-1} of data. They also included the hadronic decay of B mesons for tagging. The detailed techniques are similar to what to be explained later. The summary of the measurement of $|V_{ub}|$ can be found in Table 6. All the results are in good agreement with the results from the Belle experiment.

- Full reconstruction tag

In this method [25], Belle fully reconstructs one of the two B mesons from $\Upsilon(4S)$ decay ($B_{\rm tag}$) in one of the following hadronic decay modes, $B^- \to D^{(*)0}\pi^-$, $B^- \to D^{(*)0}\rho^-$, $B^- \to D^{(*)0}a_1^-$, $B^- \to D^{(*)0}D_s^{(*)-}$, $B^0 \to D^{(*)+}\pi^-$, $B^0 \to D^{(*)+}\rho^-$, $B^0 \to D^{(*)+}a_1^-$, or $B^0 \to D^{(*)+}D_s^{(*)-}$. As was done in other B meson analyses, decays are identified on the basis of the proximity of the beam-energy constrained mass $M_{\rm bc}$

Table 6: Summary of $|V_{ub}|$ measurements by the BaBar collaboration with different theoretical calculations.

	q^2 GeV^2/c^4	$\|V_{ub}\| \times 10^{-3}$
Ball-Zwicky	< 16	$3.2 \pm 0.2 \pm 0.1\ ^{+0.5}_{-0.4}$
HPQCD	> 16	$4.5 \pm 0.5 \pm 0.3\ ^{+0.7}_{-0.5}$
FNAL	> 16	$4.0 \pm 0.5 \pm 0.3\ ^{+0.7}_{-0.5}$
APE [24]	> 16	$4.1 \pm 0.5 \pm 0.3\ ^{+1.6}_{-0.7}$

and ΔE to their nominal values of the B meson rest mass and zero, respectively. If multiple tag candidates are found, the one with values of $M_{\rm bc}$ and ΔE closest to nominal is chosen. Events with a $B_{\rm tag}$ satisfying the selections $M_{\rm bc} > 5.27$ GeV/c^2 and $-0.08 < \Delta E < 0.06$ GeV are retained. The charge of the $B_{\rm tag}$ candidate is necessarily restricted to $Q_{\rm tag} = 0$ or $Q_{\rm tag} \pm 1$ by demanding that it is consistent with one of the above decay modes. Reconstructed charged tracks and electromagnetic clusters which are not associated with the $B_{\rm tag}$ candidate are used to search for the signal B meson decays of interest recoiling against the $B_{\rm tag}$. After all cuts to enhance the signal are applied, remaining data are projected as a function of missing mass squared ($M_{\rm miss}$), as shown in Fig. 8. As is demonstrated in the figure, a high purity signal can be obtained with this method. A preliminary branching fractions are obtained as

$$\mathcal{B}(B \to \pi^- \ell\nu) = 1.49 \pm 0.26({\rm stat}) \pm 0.06({\rm syst}) \times 10^{-4}, \quad (10)$$

$$\mathcal{B}(B \to \pi^0 \ell\nu) = 0.86 \pm 0.17({\rm stat}) \pm 0.06({\rm syst}) \times 10^{-4}. \quad (11)$$

Whilst the statistical precision of these measurements is limited at present, the potential power of the full reconstruction tagging method, when it can be used with larger accumulated B-factory data samples in the future, can clearly be seen.

4 Conclusions

We have discussed recent progress in measurements of $|V_{ub}|$. At present, the total error from the inclusive measurement is approximately 7 %. The theoretical uncertainty in it is still larger than the experimental uncertainty, but not by a lot anymore. The shape function, describing the Fermi motion of the b-quark inside the meson still remains a big issue in extracting $|V_{ub}|$, but different approaches produce consistent numerical values indicating the problem is well understood. Also, BaBar's new approach based on Leibovich, Low and Rothstein [5] may look promising in future as it has residual SF dependence only.

The exclusive measurements of $|V_{ub}|$ gives the total error to be greater than 10 % at present and the form factor is the main issue in this field. The untagged analyses

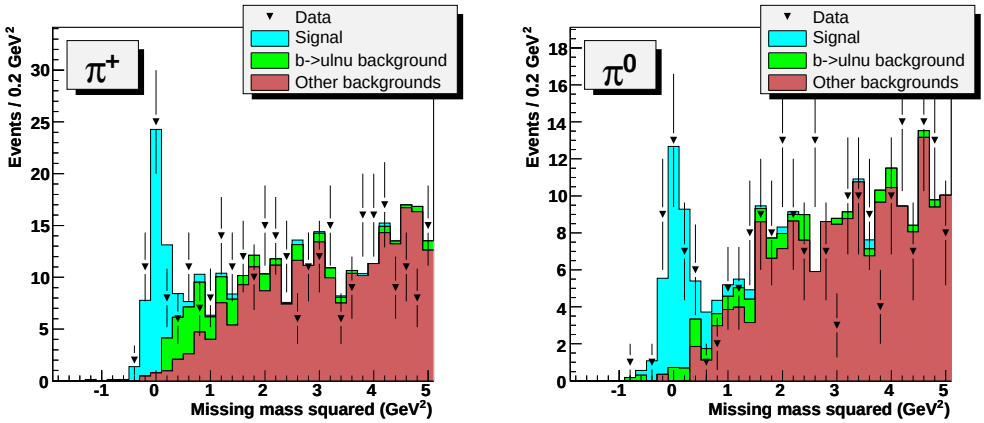

Figure 8: Missing mass squared ($M^2_{\rm miss}$) distributions after all cuts, for $B \to \pi^+\ell\nu$ on the left and $B \to \pi^0\ell\nu$ on the right. Data is indicated by the points with error bars. The blue histogram (lightest shade in greyscale) show the fitted prediction based on the LCSR model. The green histogram (middle shade in greyscale) shows the fitted $b \to u\ell\nu$ background contribution. The crimson histogram (darkest shade in greyscale) shows the fitted background contribution from other sources.

are the most precise ones at present. The theoretical uncertainty is still dominant in exclusive measurements.

I am grateful to Masahiro Morii from the BaBar experiment who kindly provided complete information on their experimental results.

Bibliography

[1] J. Chay, H. Georgi, and B. Grinstein, Phys. Lett. B **247**, 399 (1990); M. A. Shifman and M. B. Voloshin, Sov. J. Nucl. Phys. **41**, 120 (1985); I. I. Bigi *et al.*, Phys. Lett. B **293**, 430 (1992); **297**, 430(E) (1992); Phys. Rev. Lett. **71**, 496 (1993); A. V. Manohar and M. B. Wise, Phys. Rev. D **49**, 1310 (1994).

[2] N. Uraltsev, Int. J. Mod. Phys. A **14**, 4641 (1999); A. H. Hoang, Z. Ligeti, and A. V. Manohar, Phys. Rev. D **59**, 074017 (1999); T. van Ritbergen, Phys. Lett. B **454**, 353 (1999).

[3] B. O. Lange, M. Neubert and G. Paz, Phys. Rev. D **72**, 073006 (2005);

[4] J. R. Anderson and E. Gardi, J. High Energy Phys. **0601**, 097 (2006).

[5] A. K. Leibovich, I. Low and I. Z. Rothstein, Phys. Lett. B **486**, 86 (2000).

[6] The CLEO collaboration, Phys. Rev. Lett. **88**, 231803 (2002).

[7] The BaBar collaboration, Phys. Rev. D **73**, 012006 (2006).

[8] C. W. Bauer, Z. Ligeti and M. E. Luke, Phys. Rev. D **64**, 113004 (2001).

[9] The Belle collaboration, Phys. Rev. Lett. **95**, 241801 (2005).

[10] The BaBar collaboration, hep-ex/0507017.

[11] M. Neubert, Eur. Phys. J. C **40**, 165 (2005); Phys. Lett. B **612**, 13 (2005); S. W. Bosch, M. Neubert, and G. Paz, J. High Energy Phys. **11**, 073 (2004).

[12] htp://www.slac.stanford.edu/xorg/hfag.

[13] The BaBar collaboration, Phys. Rev. Lett. **96**, 222801 (2006).

[14] The HPQCD collaboration, E. Gulez *et al.*, Phys. Rev. **D73**, 074502 (2006).

[15] The FNAL collaboration, M. Okamoto *et al.*, Nucl. Phys. Proc. Suppl. **140** 461 (2005).

[16] A. Abada *et al.*, Nucl. Phys. **D619**, 565 (2001).

[17] P. Ball, R. Zwicky, Phys. Rev. **D71**, 014015 (2005).

[18] D. Scora, N. Isgur, Phys. Rev. **D52**, 2783 (1995).

[19] The CLEO collaboration, Phys. Rev. **D68**, 072003 (2003).

[20] The BaBar collaboration, hep-ex/0607060.

[21] D. Becirevic and A. B. Kaidalov, Phys. Lett. **B478**, 417 (2000).

[22] The Belle collaboration, hep-ex/0604024.

[23] The BaBar collaboration, hep-ex/0607089.

[24] A. Abada *et al.*, Nucl. Phys. **B619**, 565 (2001).

[25] The Belle collaboration, hep-ex/0610054.